



## Reduction of freely migrating defect concentrations by cascade remnants in Ni–Si alloys

A. Iwase<sup>a,b,\*</sup>, L.E. Rehn<sup>a</sup>, P.M. Baldo<sup>a</sup>, L. Funk<sup>a</sup>

<sup>a</sup> Materials Science Division, Argonne National Laboratory, 9700 S. Cass Avenue, Argonne, IL 60439, USA

<sup>b</sup> Advanced Science Research Center, Japan Atomic Energy Research Institute, Tokai-mura, Naka-gun, Ibaraki 319-11, Japan

Received 17 September 1996; accepted 22 November 1996

---

### Abstract

Interactions of cascade remnants with freely migrating defects in Ni–12.7% Si were investigated using in-situ Rutherford backscattering spectrometry during simultaneous irradiation with 1.5 MeV He and 400 keV Ne ions at elevated temperatures. Radiation induced segregation of Si atoms toward the specimen surface caused  $\gamma'$ -Ni<sub>3</sub>Si layers to grow on the surface during irradiation. The  $\gamma'$ -Ni<sub>3</sub>Si growth rate during He bombardment was strongly suppressed by simultaneous irradiation with Ne ions, even when the calculated defect production rate for the Ne ions was only a few percent of that for the He ions. This result shows that the cascade remnants generated by the Ne ions act as additional recombination sites for freely migrating defects, reducing their steady state concentration. Despite a large difference in defect properties and in the kinetics of radiation induced segregation between the two alloys, the effects of cascade remnants on freely migrating defects in Ni–12.7% Si are remarkably similar to those found previously in Cu–1% Au.

---

### 1. Introduction

It is now well established that experimentally determined production rates of freely migrating defects (FMD) are much smaller at high ( $\geq 10$  keV) recoil energies than those calculated from the modified Kinchin–Pease model or using computer simulation [1–4]. Wiedersich has examined the possible role of cascade remnants, i.e., immobile interstitial and/or vacancy clusters, in reducing FMD concentrations [5,6]. His rate-theory calculations suggested that cascade remnants, i.e., vacancy and/or interstitial clusters, generated by high-energy recoils may act as sites for significant recombination of FMD produced by other displacement events, and that such *inter-cascade* interactions might explain the apparent low values for FMD production rates measured experimentally.

Recently, large effects from cascade remnants on FMD concentrations were found experimentally in Cu–1% Au

alloys [7,8]. The large radiation induced segregation (RIS) observed in Cu–1% Au during 1.5 MeV He irradiation was dramatically suppressed under simultaneous heavy-ion irradiation, demonstrating that inter-cascade annihilation of FMD is indeed responsible for a strong reduction in FMD steady-state concentrations, as Wiedersich had predicted.

In order to examine the universality of the effect of cascade remnants on FMD concentrations, we have measured RIS in Ni–12.7% Si under simultaneous irradiation with 1.5 MeV He and 400 keV Ne ions. Si is an undersized solute in Ni, and it is believed that strong coupling of the undersized Si with the interstitial flux is responsible for the RIS of Si toward the surface seen in Ni(Si) alloys. In contrast, Au is an oversized solute element in Cu and is known to interact only weakly with interstitial defects. Also, RIS produces a depletion of Au in the near-surface during irradiation of Cu(Au) alloys at elevated temperatures, while the enrichment of Si via RIS is strong enough to produce surface coatings of  $\gamma'$ -Ni<sub>3</sub>Si even in dilute Ni(Si) alloys. In the present paper, we demonstrate that a marked reduction of the FMD concentration by cascade remnants is also observed in Ni–12.7% Si, even though

---

\* Corresponding author. Tel.: +81-292 82 5470; fax: +81-292 82 6716; e-mail: iwase@popsvr.tokai.jaeri.go.jp.

Table 1  
Irradiation parameters

Ion	Energy	$\sigma_d$ (m <sup>2</sup> )	Beam current <sup>a</sup> (nA)	Current density (A/m <sup>2</sup> )	Dpa rate (dpa/s)
He	1.5 MeV	$1.0 \times 10^{-22}$	100	$1.03 \times 10^{-1}$	$6.4 \times 10^{-5}$
Ne	400 keV	$2.2 \times 10^{-20}$	0.10	$1.37 \times 10^{-5}$	$1.9 \times 10^{-6}$
			0.25	$3.54 \times 10^{-5}$	$4.9 \times 10^{-6}$

<sup>a</sup> Through a 1 mm and a 3 mm diameter aperture, for He ions and Ne ions, respectively.

the RIS kinetics and defect properties in Ni–12.7% Si are quite different from those found in Cu–1% Au.

## 2. Experimental procedure

Rutherford backscattering spectrometry (RBS) was employed to determine the amount of RIS of Si atoms to the surface of a Ni–12.7 at% Si alloy during 1.5 MeV He single-beam irradiation, and during simultaneous dual-beam irradiation with He and 400 keV Ne ions. Detailed descriptions of the experimental procedure, including a schematic of the experimental arrangement for simultaneous irradiation, are given in a previous paper [8].

The specimen temperature was maintained at 500 or 600(±10)°C during irradiation and RBS measurement. The projected ranges for 1.5 MeV He and 400 keV Ne were 2.0 μm and 310 nm, respectively, while the measured Si-enrichment due to RIS extended to a depth of approximately 40 nm. Ion energies, beam currents through the 1 mm and 3 mm diameter apertures, respectively, for the He and Ne ions, and the total beam current densities for the present experiments, are listed in Table 1. This table also gives the cross sections for Frenkel pair production,  $\sigma_d$ , which were calculated using the TRIM-92 computer code, and the corresponding calculated displacement rates in the near-surface region for all irradiations. An average displacement threshold energy of 33 eV was assumed [9].

The weighted-average recoil energy,  $T_{1/2}$ , is defined as the displacement energy above (or below) which one-half of the defects are created. This parameter, which is frequently used to provide a simple description of defect production, is ~2 keV for the 1.5 MeV He and ~11 keV for the 400 keV Ne irradiations of the Ni–12.7% Si specimens. The Ne ions therefore produce predominantly energetic displacement cascades, while the He ions, with their relatively low  $T_{1/2}$ , generate FMD efficiently.

The results for simultaneous irradiation of the Cu–Au alloy reveal that the inert gas atoms (Ne and Ar) which accumulate in the specimen enhance the suppression of RIS [8]. To minimize this effect in the present study of Ni–12.7% Si, the Ne beam currents were chosen to be substantially smaller than were used in the Cu–Au studies. As in the previous work, we also examined the effects of

pre-irradiation with Ne, and annealing at 600 and 725°C on subsequent RIS behavior.

## 3. Experimental results

Fig. 1 shows RBS spectra acquired at 500°C from a Ni–12.7% Si specimen before and after irradiation with 1.5 MeV He ions to a calculated dose of 0.7 dpa. The reduction in the Ni RBS yield seen near the Ni leading edge (~ channel 920), and the corresponding increase in the Si yield behind the Si leading edge (~ channel 680), are clearly seen. These changes show that the Ni concentration decreases, and the Si concentration increases, in the near-surface region as a result of the irradiation. Previous studies using RBS, transmission electron microscopy, and Auger electron spectroscopy have shown that the redistribution of Ni and Si atoms during irradiation can be attributed to the nonequilibrium RIS of Si atoms toward the surface, and the subsequent precipitation of the  $\gamma'$ -Ni<sub>3</sub>Si phase [10].

RIS is caused by the existence of a persistent flux of freely migrating defects, and a preferential coupling of the undersized Si atoms to this flux. The amount of Si RIS toward the surface, i.e., the thickness of the  $\gamma'$  layer, can be readily determined by taking the difference between the

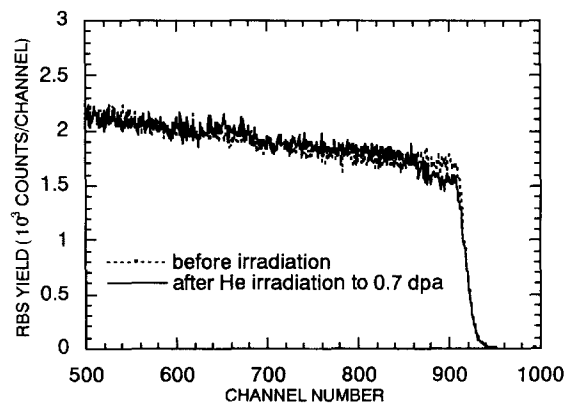


Fig. 1. RBS spectra for 1.5 MeV He incident on Ni–12.7% Si before (dashed line) and after (solid line) 1.5 MeV He irradiation to a calculated near-surface dose of 0.7 dpa.

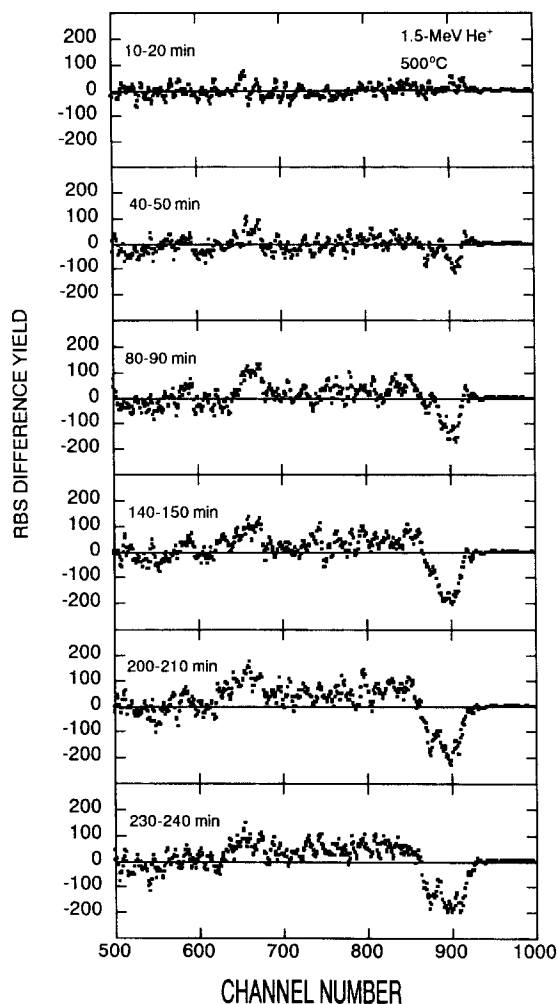


Fig. 2. Series of RBS difference spectra acquired during 1.5 MeV He irradiation at 500°C.

RBS spectra for the irradiated and unirradiated specimens. The reduction in RBS yield near the Ni edge, or equivalently, the increase near the Si edge, is directly proportional to the magnitude of the RIS.

A sequence of such RBS difference spectra acquired during He-only irradiation (100 nA through the 1 mm diameter aperture) at 500°C is displayed in Fig. 2. Before calculating the difference spectra, all as-acquired RBS spectra were first normalized to 2000 counts per channel just in front of the Si edge. As done previously [1], the area of negative RBS yield near the Ni leading edge was then used to determine the thickness of the radiation-induced  $\gamma'$ -Ni<sub>3</sub>Si layers because the relative change there is significantly greater than that which occurs below the Si edge. The conversion to thickness was made using an atomic density of  $9.3 \times 10^{28}$  atoms/m<sup>3</sup> for  $\gamma'$ -Ni<sub>3</sub>Si.

In Fig. 3, the thicknesses of the  $\gamma'$  layers measured during He irradiation at 500 and 600°C are plotted as a

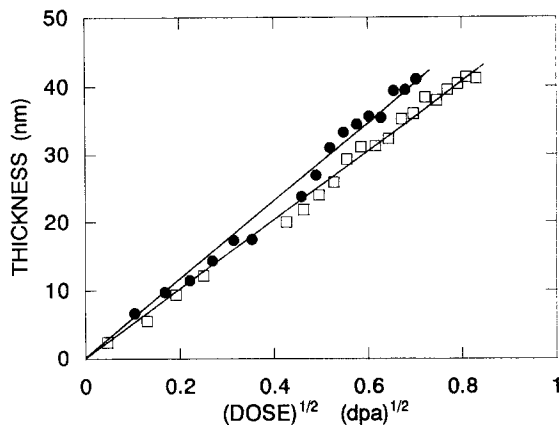


Fig. 3. Growth rates for Ni<sub>3</sub>Si  $\gamma'$ -films on Ni–12.7% Si during irradiation with 1.5 MeV He ions at 500°C (open squares) and 600°C (solid circles); the calculated dose rate is  $6.4 \times 10^{-5}$  dpa/s.

function of the square root of the calculated dpa (displacements per atom). These data reveal that the  $\gamma'$  layer thickness is directly proportional to the square root of the

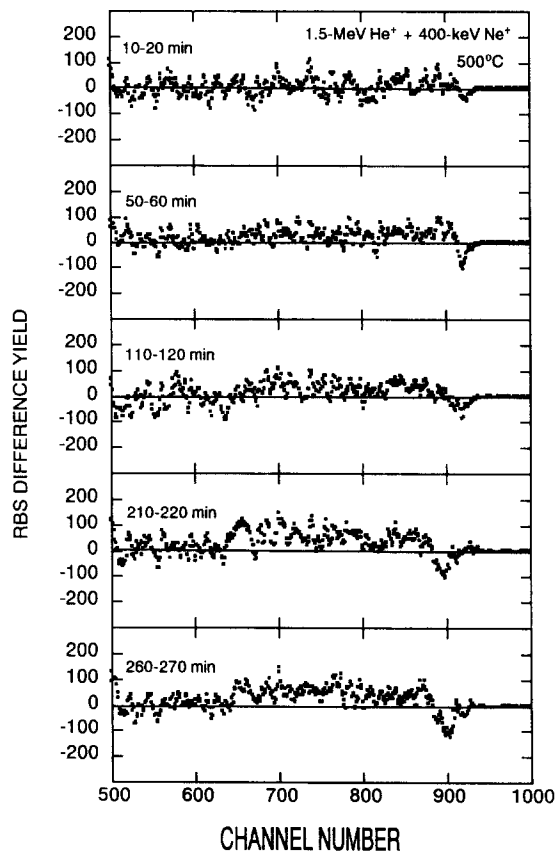


Fig. 4. A series of RBS difference spectra acquired during simultaneous irradiation with 1.5 MeV He and 400 keV Ne (0.1 nA). Irradiation temperature is 500°C.

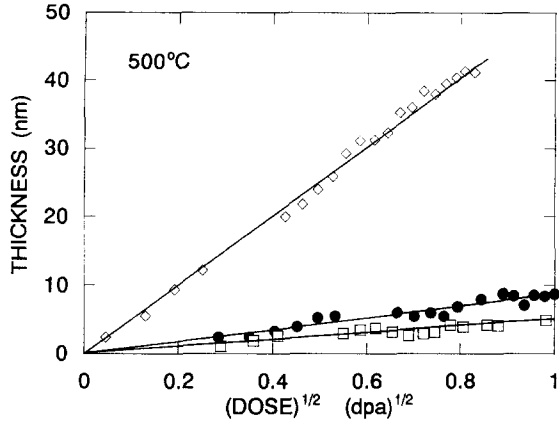


Fig. 5. Growth rates measured for Ni<sub>3</sub>Si γ'-films on Ni-12.7% Si at 500°C plotted as a function of the square root of the calculated dpa for 1.5 MeV He-only irradiation (open diamonds), and simultaneous irradiation with He and Ne (solid circles - 0.1 nA Ne; open squares - 0.25 nA Ne). For simultaneous irradiation, the abscissa represents the sum of the dpa from both beams.

calculated dpa, and that the growth rate is approximately 50 (60) nm/dpa<sup>1/2</sup> for He irradiation at 500 (600)°C. These He-only irradiation growth rates agree well with those obtained previously [1,11].

Fig. 4 displays a sequence of RBS difference spectra acquired during simultaneous irradiation at 500°C with 1.5 MeV He and 400 keV Ne (0.1 nA through the 3 mm diameter aperture). We see immediately that the negative RBS yield differences near the Ni leading edge are much smaller for simultaneous irradiation than for He-only irradiation. The corresponding γ' layer thicknesses for simultaneous irradiation with He and Ne (solid circles, 0.1 nA Ne; open squares, 0.25 nA Ne) acquired at 500 and 600°C are plotted as a function of the square root of the calculated dpa in Figs. 5 and 6, respectively. For comparison, the results for the He-only irradiation are also shown.

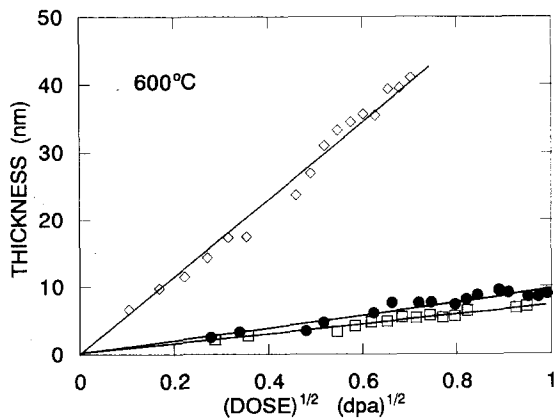


Fig. 6. Same as Fig. 5 except that the irradiation temperature is 600°C.

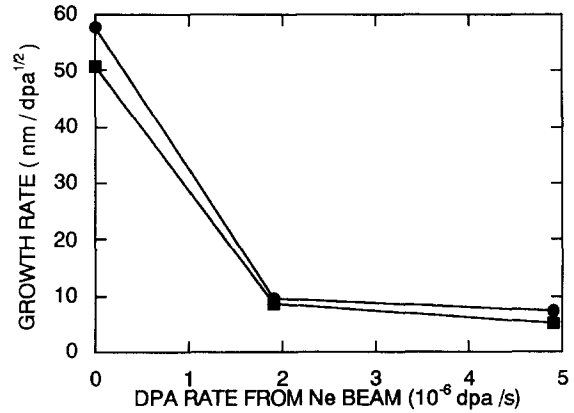


Fig. 7. Growth rate of Ni<sub>3</sub>Si γ'-layers during He + Ne simultaneous irradiation as a function of the dpa calculated for the Ne ion beam. The irradiation temperatures are 500°C (solid squares) and 600°C (solid circles).

For the simultaneous irradiations, the abscissa represents the square root of the sum of the dpa calculated for both beams. However, the square root of the total dpa,  $\sqrt{\Phi^{\text{cal}}}$ , for simultaneous irradiation is only slightly (1.04 and 1.02 times) larger than that from the He beam, since the dpa rates for the Ne are only 8% and 3% of that for the He. As can be seen in Figs. 5 and 6, during the simultaneous irradiation as well as the He-only irradiation, the layer thickness,  $W$ , is directly proportional to the square root of the calculated dpa, i.e.,

$$W = A\sqrt{\Phi^{\text{cal}}} \quad (1)$$

The growth rate constants,  $A$ , measured for the simultaneous irradiations, are plotted as a function of the calculated dpa rates for the Ne beams in Fig. 7. About an order of magnitude decrease is observed in the growth rate between the He-only and the He + Ne simultaneous irradiation.

In order to examine the thermal stability of the cascade remnants responsible for the observed suppression of RIS, we next compare the γ'-layer growth rate under simultaneous irradiation with that obtained following pre-irradiation experiments. Three specimens were first irradiated with 400 keV Ne at 500°C; the irradiation time was 1 h and the beam current through the 3 mm diameter aperture was 1.0 nA. One pre-irradiated specimen was then irradiated with 1.5 MeV He at 500°C. The measured growth rate is shown in Fig. 8, along with the growth rates for He-only and He + Ne (0.25 nA) simultaneous irradiation. Note that although some γ' forms on the surface as a result of the pre-irradiation treatment, the data for all three irradiation runs shown here begin at the origin (0 dpa), so that the relative growth rates can be readily compared.

The irradiation time for simultaneous irradiation was about 4 h and the Ne beam current was 0.25 nA. Hence the total dpa from the Ne irradiation, as well as the concentration of implanted Ne ions, are approximately the same for

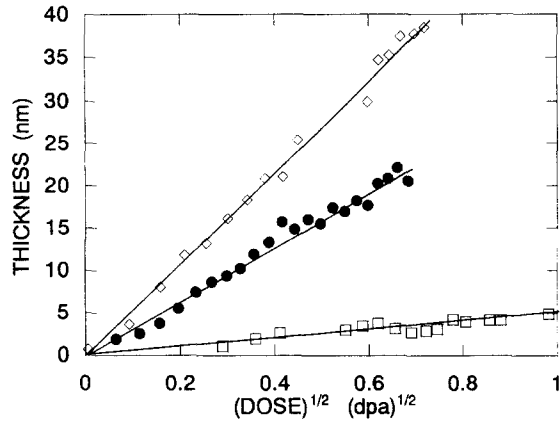


Fig. 8. Effect of pre-irradiation with 400 keV Ne to 0.07 dpa on the growth rate of the  $\gamma'$ -layer (solid circles). Growth rates for irradiation with He-only (open diamonds), and simultaneous He and Ne (0.25 nA) (open squares) are also plotted. The pre-irradiation and RBS measurement temperature was 500°C.

the simultaneous irradiation and the pre-irradiation runs. However, the measured growth rates are quite different. There is a clear suppression of the RIS following pre-irradiation, but it is not nearly as strong as the suppression observed during simultaneous bombardment. The growth rate observed during simultaneous irradiation is only  $\sim 15\%$  of that found after pre-irradiation.

The two other specimens pre-irradiated with Ne at 500°C were annealed at 600 and 725°C, respectively. They were both subsequently irradiated with 1.5 MeV He at 500°C and the growth of the  $\gamma'$  layers was measured. The

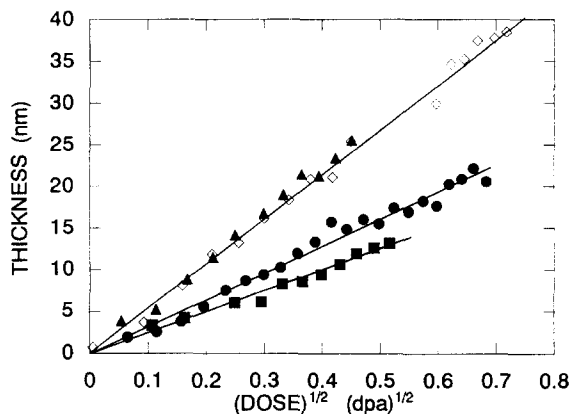


Fig. 9. Effect of annealing on the subsequent  $\gamma'$ -layer growth rate in Ni-12.7% Si pre-irradiated with Ne. Without pre-irradiation (open diamonds), pre-irradiated with Ne to 0.07 dpa (solid circles), pre-irradiated with Ne to 0.07 dpa and subsequently annealed at 600°C for 1 h (solid squares), and pre-irradiated with Ne to 0.07 dpa and subsequently annealed at 725°C for 1 h (solid triangles). Temperatures for pre-irradiation and RBS measurements are all 500°C.

results of these annealing experiments are shown in Fig. 9. Essentially no recovery of the growth rate is observed after annealing at 600°C. However, the suppression of the RIS found after pre-irradiation at 500°C disappears essentially completely after annealing at 725°C.

#### 4. Discussion

The experimental results (Figs. 4–7) presented in Section 3 demonstrate clearly that simultaneous Ne irradiation strongly suppresses the He-irradiation-induced segregation of Si toward the surface. Since FMD are what drive the RIS, these results indicate that the steady-state concentration of FMD is reduced during simultaneous Ne irradiation. This reduction in FMD concentration due to simultaneous Ne irradiation can be explained by the same mechanism invoked to account for the previous Cu-1% Au results [7,8]. That is, cascade remnants generated within the energetic cascades from the Ne irradiation introduce efficient recombination sites for FMD produced by the He beam, reducing their steady-state concentrations.

Some information on the stability of the cascade remnants responsible for the reduction of the FMD concentration can be extracted from the results of the pre-irradiation experiments. For example, the cascade remnants introduced by pre-irradiation with Ne at 500°C (Fig. 8) reduce the  $\gamma'$  layer growth rate to  $\sim 65\%$  of that found during He-only irradiation. In comparison, the growth rate under He + Ne simultaneous irradiation is only 10% of that found during He-only irradiation. Hence simultaneous irradiation is substantially more effective at 500°C in suppressing RIS than is pre-implantation, indicating that the vacancy and interstitial clusters responsible for the suppression are unstable in this temperature range. This observation is consistent with earlier TEM observations [12] which showed that the number of visible defects in ion-irradiated Ni decreases strongly for irradiation temperatures above 500°C, i.e., much of the cascade damage in Ni is thermally unstable above 500°C.

The pre-irradiation results in Fig. 9 indicate that a substantial fraction of the RIS suppression by pre-implantation should be attributed to those cascade remnants which survive annealing at 600°C, since the main contribution to the reduction of FMD concentration comes from those cascade remnants which disappear after annealing between 600 and 725°C.

In the present report, and in our previous papers [7,8], we have demonstrated that the interactions of FMD with cascade remnants generated by energetic recoils cause a strong reduction of steady-state FMD concentrations in Cu-1% Au and Ni-12.7% Si. The similarity in the effects of metastable cascade remnants on FMD concentrations for two alloys with quite different RIS kinetics, and defect

properties, implies that the inter-cascade annihilation of FMD is a general concept, one useful for understanding the apparent small FMD production efficiencies found at recoil energies  $> 10$  keV.

### 5. Summary

Using simultaneous irradiation of Ni–12.7% Si with 1.5 MeV He and 400 keV Ne, and in-situ RBS measurements, we have found that the cascade remnants generated by Ne ions act as efficient annihilation sites for FMD, resulting in the reduction of the steady-state concentrations of FMD. Thermally unstable defect clusters, which are generated within energetic cascades during irradiation, are responsible for the observed reduction. Despite having quite different RIS kinetics and defect properties, the inter-cascade annihilation of FMD in Ni–12.7% Si appears quite similar to that observed previously in Cu–1% Au.

### Acknowledgements

We are grateful to H. Wiedersich and P.R. Okamoto for fruitful discussions throughout the course of this work. The expert assistance with specimen preparation of B. Kestel, and stimulating discussions with T. Hashimoto and H. Abe are also acknowledged. This work was supported by the

U.S. Department of Energy, BES-Materials Science Contract No. W-31-109-ENG-38.

### References

- [1] L.E. Rehn, P.R. Okamoto and R.S. Averback, *Phys. Rev. B* 30 (1984) 3073.
- [2] T. Hashimoto, L.E. Rehn and P.R. Okamoto, *Phys. Rev. B* 38 (1988) 12868.
- [3] R.A. Erck and L.E. Rehn, *J. Nucl. Mater.* 168 (1989) 208.
- [4] A. Muller, V. Naundorf and M.-P. Macht, *J. Appl. Phys.* 64 (1988) 3445.
- [5] H. Wiedersich, *Mater. Sci. Forum* 97–99 (1992) 59.
- [6] H. Wiedersich, *J. Nucl. Mater.* 205 (1993) 40.
- [7] A. Iwase, L.E. Rehn, P.M. Baldo and L. Funk, *Appl. Phys. Lett.* 67 (1995) 229.
- [8] A. Iwase, L.E. Rehn, P.M. Baldo and L. Funk, *J. Nucl. Mater.* 238 (1996) 224.
- [9] P. Lucasson, in: *Proceedings of the International Conference on Fundamental Aspects of Radiation Damage in Metals*, Gatrinburg, TN, United States Energy Research and Development Agency, CONF-751006-p1, Vol. 1 (GPO, Washington, DC, 1976) p. 42.
- [10] L.E. Rehn and P.R. Okamoto, in: *Phase Transformations during Irradiation*, ed. F.V. Nolfi, Jr. (Applied Science Publishers, London, 1982) p. 247.
- [11] R.S. Averback, L.E. Rehn, W. Wagner, H. Wiedersich and P.R. Okamoto, *Phys. Rev. B* 28 (1983) 3100.
- [12] T.M. Robinson and M.L. Jenkins, *Philos. Mag. A* 43 (1981) 999.